Supercurrent fluctuations in filaments

Jorge Berger*
Department of Physics and Optical Engineering, Ort Braude College, P.O. Box 78, 21982 Karmiel, Israel
(Received 6 October 2011; revised manuscript received 21 March 2012; published 5 April 2012)

We evaluate the average and the standard deviation of the supercurrent in superconducting nanobridges, as functions of temperature, phase difference, and sample parameters, in an equilibrium situation. We also evaluate the autocorrelation of the supercurrent as a function of the elapsed time. The behavior of supercurrent fluctuations is qualitatively different from that of the normal current: they depend on the phase difference, have a different temperature dependence, have nonzero averages, and for an appropriate range their standard deviation is independent of the probing time. We considered two radically different filaments and obtained very similar results for both. Fluctuations of the supercurrent can in principle be measured.

DOI: 10.1103/PhysRevB.85.144507 PACS number(s): 74.40.−n, 74.78.Na, 72.70.+m

I. INTRODUCTION

Josephson junctions are of common use in many technological devices and their behavior as a circuit element is described in textbooks;[1–3] the influence of thermal fluctuations on the normal current is described as Johnson noise. The voltage due to thermal noise was studied by Ivanchenko and Zil'berman[4] and by Ambegaokar and Halperin.[5]

In this study we are interested in the equilibrium fluctuations of the supercurrent. Since supercurrent is actually an equilibrium variable rather than a diffusion process, we may expect—and will indeed find—that its fluctuations are qualitatively different from those of the normal current. Early works on fluctuations in junctions[6] state that there is no noise in supercurrent to quadratic order in the temperature. On the other hand, Averin and Imam[7] found that supercurrent fluctuations in mesoscopic contacts are large on the scale of the classical shot noise.

The kind of junction considered in this article is a filament close to the critical temperature, which can be described by means of the Ginzburg-Landau model. If the entire filament has a critical temperature that is above the experimental temperature T, the filament may be regarded as a constriction; if parts of the filament have a critical temperature below T, it may be regarded as a superconductor-normal metal-superconductor (SNS) junction. In the case where fluctuations are ignored, the junction-like behavior of a filament has been studied for static[8] and for dynamic[9] situations.

The situation we will study here is a case of dynamic equilibrium. We will consider a superconducting filament that bridges between two "banks." At the banks fluctuations are negligible and the order parameter will have fixed equilibrium values, whereas along the filament the order parameter and the electromagnetic potential fluctuate. In the absence of fluctuations, the current along the filament would be given by the current-phase relation.

II. METHOD AND DEFINITIONS

We will use the time-dependent Ginzburg-Landau (TDGL) equations with Langevin terms, which will be handled numerically by means of finite differences. We have described this method in detail in the past[10,11] and shown good agreement with statistical mechanics and with experiments. The Langevin method states the following: if a system has an equilibrium temperature T and a variable Q which in the absence of thermal fluctuations follows an evolution $Q(t+\tau) = Q(t) - (\Gamma_Q \partial G/\partial Q)\tau$, where τ is a short lapse of time, G the energy of the system, and Γ_Q a relaxation constant, then, when fluctuations are taken into account, $Q(t+\tau) = Q(t) - (\Gamma_Q \partial G/\partial Q)\tau + \eta_Q$, where η_Q is a random variable with zero average, normal distribution, and variance

$$\langle \eta_Q^2 \rangle = 2\Gamma_Q k_B T \tau \ , \tag{1}$$

where k_B is the Boltzmann constant.

For a one-dimensional filament we define the gauge-invariant order parameter $\tilde{\psi}(x) = \exp[(2\pi i/\Phi_0)\int_0^x A(x')dx']\psi(x)$, where x is the arc length, ψ the "canonical" order parameter, A the tangential component of the vector electromagnetic potential, and Φ_0 the quantum of flux. In the absence of fluctuations, the 1D-TDGL equation can be written as[12]

$$\eta\hbar \frac{\partial \tilde{\psi}}{\partial t} = -\left[\alpha + \beta|\tilde{\psi}|^2 - \frac{\hbar^2}{2m}\frac{\partial^2}{\partial x^2} - \frac{1}{w}\frac{\partial w}{\partial x}\frac{\partial}{\partial x} - \frac{2\pi i \eta \hbar}{\Phi_0}\int_0^x \frac{\partial A}{\partial t}(x')dx'\right]\tilde{\psi} \ , \tag{2}$$

where m is the mass of a Cooper pair, $w(x)$ the cross section of the filament, and η, α, and β are material parameters; the sign of α determines whether the local critical temperature T_c is above or below T. TDGL is valid only close to T_c and not far from equilibrium;[13,14] since we are anyway interested in fluctuations that are important only close to T_c, this is not a real limitation for our purpose.

Thermal fluctuations are added to Eq. (2) in two steps:[10] a Langevin term is added to account for fluctuations of $\psi(x)$, and then the phase of $\tilde{\psi}(x)$ is modified in order to account for fluctuations of $A(x')$ (i.e., Johnson noise). In Ref. 10 it is shown that both ψ and A behave as the variable Q in Eq. (1). The current along the filament is obtained from the requirement[11] that the phase difference between the banks remains fixed.

We will take the boundary conditions $\tilde{\psi}(0,t) = \sqrt{-\alpha(0)/\beta(0)}$, $\tilde{\psi}(L,t) = \sqrt{-\alpha(L)/\beta(L)}\exp(i\gamma)$, where L is the length of the filament; γ is the gauge-invariant phase difference. The normal current $I_N(x,t)$ and the supercurrent $I_S(x,t)$ are not separately constant along the filament. We define the supercurrent as the weighted average $I_S(t) =$

$\int_0^L I_S(x,t)w(x)^{-1}dx/\int_0^L w(x)^{-1}dx$. $w(x)^{-1}$ appears as a natural weight in Refs. 10,11; in this work we consider uniform cross section only, so that this weight and the fourth term in Eq. (2) can be ignored. We define dimensionless sample parameters that characterize the filament:

$$\tilde{\alpha} = \alpha m L^2/\hbar^2, \quad \tilde{\beta} = \beta m L/\hbar^2 w, \quad \tilde{R} = 4e^2\eta L/\hbar\sigma w, \qquad (3)$$

where e is the electron charge and σ is the electrical conductivity.

Using BCS, dirty limit,[1] and free electron gas approximations, the geometric parameters for a uniform filament can be expressed in terms of the sample parameters, $T - T_c$, and microscopic parameters. We obtain

$$L^2 = \pi\hbar^2 k_F \ell_e \tilde{\alpha}/6mk_B(T - T_c), \quad w = 0.51L/n_e\ell_e^2\tilde{\beta}, \qquad (4)$$

where k_F is the Fermi wave vector, ℓ_e the mean free path, and n_e the electron density. Within these approximations we also have $\eta = 3/4k_F\ell_e$.

III. RESULTS

We have examined two situations. The first (Sec. III A) is that of filaments with uniform superconductivity; in the second case (Sec. III B) the middle of the filament is nominally normal. The filament was divided into 30 computational cells and evolution was followed in steps of duration $1.3 \times 10^{-4}\eta m L^2/\hbar$. The first 10^7 steps had the purpose of relaxation to typical values of $\tilde{\psi}$ and then 12×10^7 steps were used for averaging. Changing the time step by an order of magnitude typically leads to changes in the average current that are smaller than 5%; the influence of the number of computational cells is discussed in the Appendix. The averages shown in the figures are averages over time and I_{S0} denotes the supercurrent in the absence of thermal fluctuations.

A. Uniform filament

1. Fluctuation-temperature dependence

In this section we take $-\tilde{\alpha} = \tilde{\beta} = \tilde{R} = 1$ and study the influence of temperature. It should be emphasized that the temperature is always very close to T_c, so that the fluctuation temperature is a conceptual entity. Operationally, the fluctuation temperature is a value of T that we set into Eq. (1) as a control of the fluctuation strength. When we report on the value of I_S for $T = 0$, what we mean is the value that would be obtained in the absence of fluctuations. The main motivation for studying the influence of T is the comparison with the fluctuations of the normal current, which have a variance proportional to T.

If temperature is varied in an experiment with a fixed sample, this mainly affects the value of $\tilde{\alpha}$. If the experimentalist really wants to change the effective value of T, two strategies seem possible. One of them is electrostatic tuning of T_c, as implemented with a ferromagnetic layer;[15] another possibility is repetition of the experiment with samples that have different critical temperatures (or different lengths, since the influence of temperature scales as L^2). Although measurements for several values of T while keeping fixed values of the sample parameters would be experimentally demanding, in the absence of available data we consider it instructive to study the trends due to the separate variations of each of the parameters in the theory.

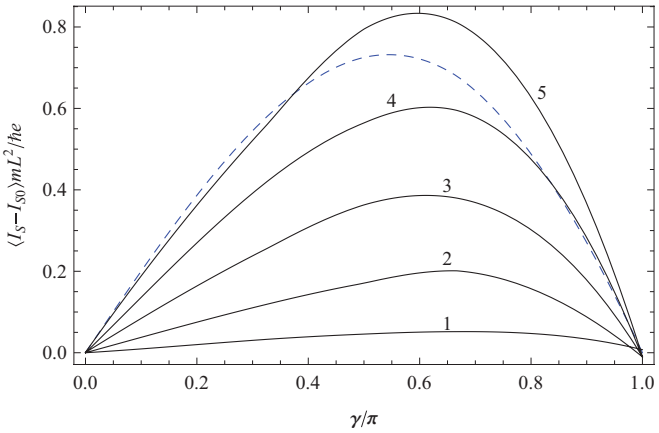

FIG. 1. (Color online) Average deviation of the supercurrent from the value that would be obtained without thermal fluctuations, as a function of the phase difference and for $\alpha = -\hbar^2/mL^2$, $\beta = \hbar^2 w/mL$, $\tilde{R} = 1$ and several values of the fluctuation temperature T (solid curves). $T = 0.1n^2\hbar^2/mL^2k_B$, where n is the number marked next to each curve. For comparison, we have also drawn the curve $-I_{S0}/3$ (dashed line).

Figure 1 shows the average deviation of I_S from I_{S0} as a function of γ, for several values of T. We see that fluctuations not only lead to variance of the supercurrent, as in the case of normal current, but also lead to a shift of the average value. I_S and I_{S0} are negative for $0 < \gamma < \pi$, so that $|\langle I_S\rangle| < |I_{S0}|$. For a material with critical temperature of the order of 1 K, the highest temperature in Fig. 1 corresponds to a filament length of the order of 30 nm and the highest current deviation, to the order of 10 nA. The γ dependence of $\langle I_S\rangle - I_{S0}$ has some resemblance to that of I_{S0}, which has been included in the figure for comparison. Figure 2 presents $\langle I_S\rangle - I_{S0}$ as a function of T; it is apparent that this deviation behaves differently for different values of γ.

Figure 3 shows the standard deviation of I_S as a function of γ. Note that whereas the standard deviation of Johnson noise is inversely proportional to the square root of the probing time

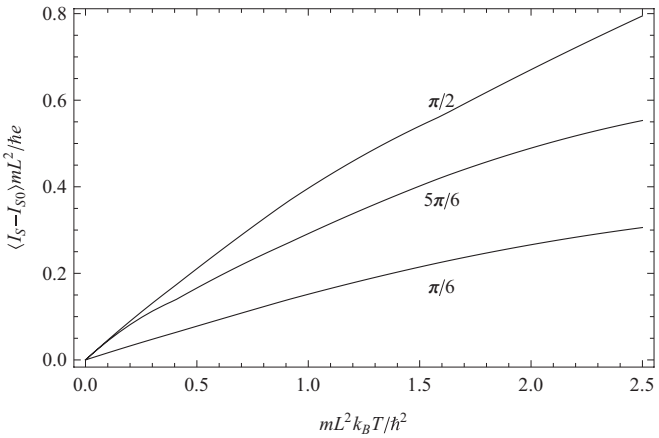

FIG. 2. Deviation of the supercurrent from the fluctuation-free value, as a function of the fluctuation temperature and for several phase differences, marked next to each curve.

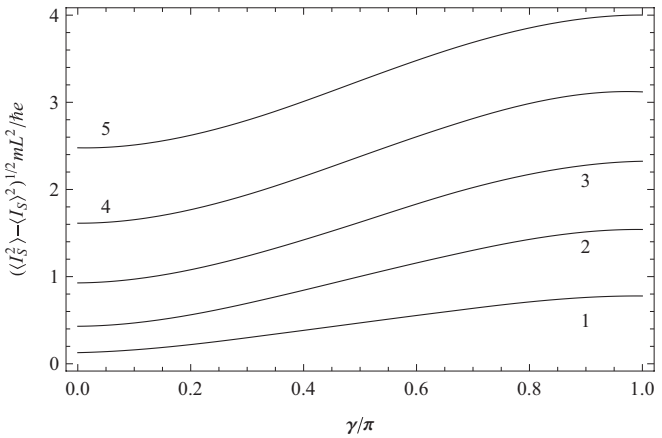

FIG. 3. Standard deviation of the supercurrent, as a function of the phase difference, for several values of T. The temperatures and sample parameters are the same as in Fig. 1.

(provided that it is long compared to $\hbar/k_BT$), the standard deviation of I_S is independent of the probing time (provided that it is short compared to the decoherence time that we will find below). In addition, the standard deviation of I_S depends on the phase difference, whereas that of I_N does not. On the other hand, the present result does not support the scenario assumed in Ref. 16, according to which fluctuations of the order parameter just scale the supercurrent, while the shape of the current-phase relation remains fixed; if this were the case, the standard deviation of I_S would be proportional to I_{S0}.

Figure 4 shows the temperature dependence of the standard deviation of I_S. Whereas for the normal current the standard deviation is proportional to $T^{1/2}$, no similar scaling is found for the supercurrent. Proportionality seems to occur in the case $\gamma=\pi$, but this is only approximate.

Figure 5 shows the autocorrelation of the supercurrent, $K(t')=[\langle I_S(t+t')I_S(t)\rangle-\langle I_S\rangle^2]/(\langle I_S^2\rangle-\langle I_S\rangle^2)$ for $0\leqslant\gamma\leqslant\pi$. We see that the smaller the value of γ, the shorter the typical time required to "forget" a previous value of I_S. The inset shows the spectral density $J(\omega)=(1/\pi)\int_0^\infty K(t)\cos(\omega t)dt$.

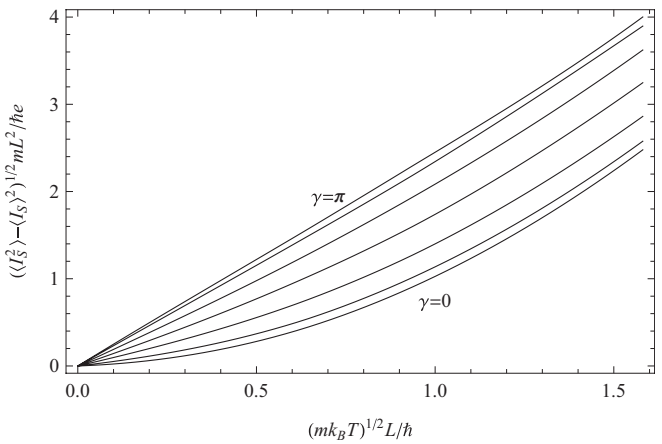

FIG. 4. Dependence of the standard deviation of the supercurrent on the fluctuation temperature. The lowest curve is for $\gamma=0$, the highest for $\gamma=\pi$, and the curves in between are in steps of $\pi/6$.

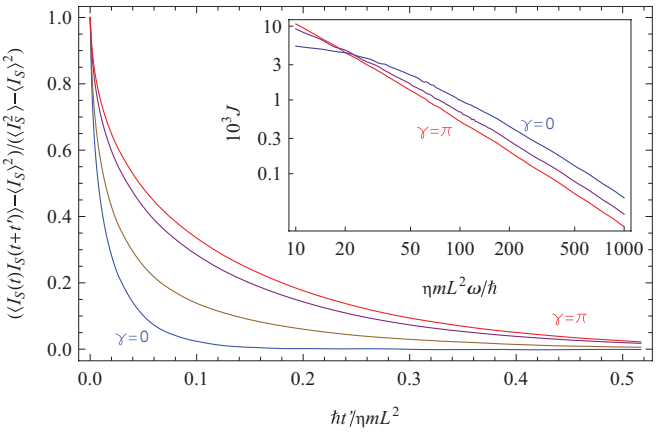

FIG. 5. (Color online) Autocorrelation function of I_S, as a function of the elapsed time t', for $T=2.5\hbar^2/mL^2k_B$ and $\gamma=n\pi/3$, $n=0,1,2,3$. The other parameters are as in Fig. 1. Inset: spectral density for $\gamma=0,\pi/2,\pi$.

If I_S is measured many times, each time during a probing period of length τ such that $K(\tau)\sim 1$, then each measurement can essentially be regarded as instantaneous and the standard deviation of I_S is given by Fig. 3, with practically no τ dependence; if $K(\tau)\sim 0$, then fluctuations of I_S essentially become white noise and the standard deviation of I_S should decrease as $\tau^{-1/2}$. According to Fig. 5, the crossover value of τ (the "decoherence time") increases with γ and is of the order of $0.1\eta mL^2/\hbar$ (for $L\sim 1$ μm and $k_F\ell_e\sim 10$, this is of the order of 10^{-10} s).

The faster relaxation of fluctuations for small γ is counterintuitive, since according to Fig. 3 the influence of thermal agitation is stronger for large γ, and we might expect this agitation to destroy any particular configuration of the order parameter that results in a particular supercurrent at a given time. Figure 6 shows that the γ dependence of the relaxation times of I_S is not dominated by thermal agitation, but rather by the fluctuationless dynamics. At $T\sim 0$, memory loss of particular configurations is faster for small γ; thermal agitation

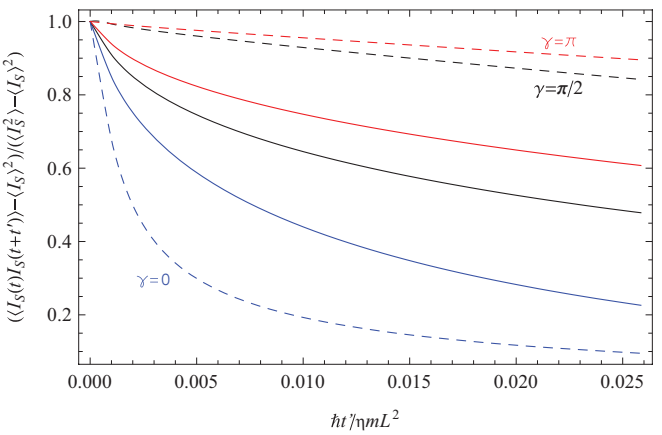

FIG. 6. (Color online) Influence of fluctuations on the autocorrelation function. The dashed lines are for $T\sim 0$ and the continuous lines for $T=2.5\hbar^2/mL^2k_B$. The lower (blue) lines are for $\gamma=0$, the middle lines for $\gamma=\pi/2$, and the upper (red) lines for $\gamma=\pi$.

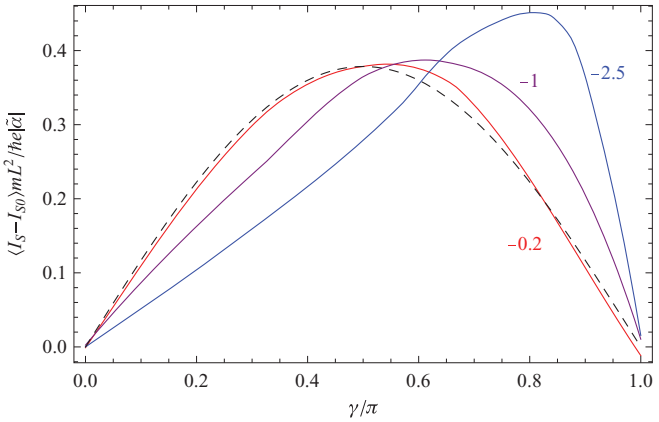

FIG. 7. (Color online) Deviation of the supercurrent from the fluctuationless value as a function of the phase difference for several values of $\tilde{\alpha}$, marked next to each curve. $T = 0.9\hbar^2/mL^2k_B$, $\beta = \hbar^2 w/mL$, $\tilde{R} = 1$. The dashed line has sinusoidal shape and is included for comparison.

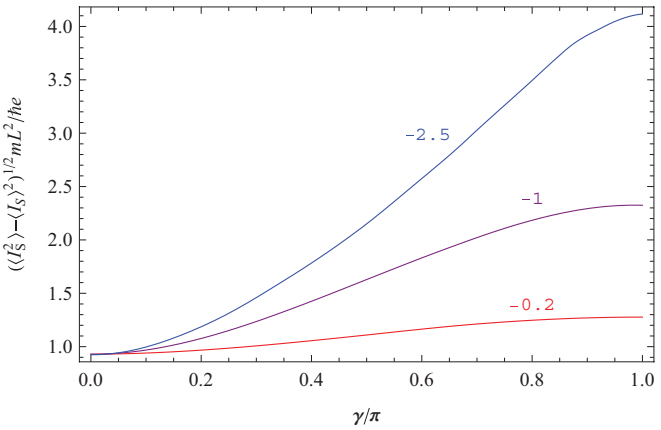

FIG. 8. (Color online) Standard deviation of the supercurrent, as a function of the phase difference, for several values of $\tilde{\alpha}$; same parameters as in Fig. 7.

moderates the γ dependence. It is interesting to note that in the case $\gamma = 0$ thermal agitation leads to delay of the relaxation.

The results in Figs. 3 and 6 can be interpreted as follows. In the case $\gamma = 0$ the order parameter is pinned with the same phase at both boundaries, giving a large energy advantage to a uniform order parameter all along the filament. Therefore, the system is comparatively rigid: deviations from the equilibrium configuration are small and return to equilibrium is fast. In the case $\gamma = \pi$ the order parameter is pinned with opposite phases at the boundaries, so that the system is frustrated and comparatively indifferent; as a consequence, deviations from equilibrium are large and return to it is slow.

2. *Influence of sample parameters*

Variation of $\tilde{R}$ by an order of magnitude has only a minor influence on the supercurrent. In the following we report on the influence of variations of $\tilde{\alpha}$ and $\tilde{\beta}$.

Figure 7 shows the deviation of I_S from its fluctuationless value for several values of $\tilde{\alpha}$. The typical sizes of $\langle I_S - I_{S0}\rangle$ are roughly proportional to $\tilde{\alpha}$. For $|\tilde{\alpha}| \ll 1$ this deviation has a sinusoidal shape; as $|\tilde{\alpha}|$ increases, its maximum moves to larger values of γ.

Figure 8 shows the standard deviation of I_S for the same values of $\tilde{\alpha}$ as in Fig. 7. We find that for $\gamma = 0$ this standard deviation is independent of $\tilde{\alpha}$, whereas for $\gamma = \pi$ it increases with $|\tilde{\alpha}|$.

The inset in Fig. 9 shows the behavior of $\langle I_S - I_{S0}\rangle$ for several values of $\tilde{\beta}$. As could be expected, the influence of increasing $\tilde{\beta}$ is qualitatively similar to that of decreasing $|\tilde{\alpha}|$, but far more moderate. Figure 9 shows the influence of $\tilde{\beta}$ on the standard deviation of I_S; again, the influence is qualitatively opposed to that of $|\tilde{\alpha}|$, but variation of $\tilde{\beta}$ does have an effect for $\gamma = 0$.

Figure 10 shows the standard deviation of the supercurrent as a function of temperature, for $\gamma = 0$ and $\gamma = \pi$, and for several values of $\tilde{\alpha}$ and $\tilde{\beta}$. As already mentioned, for $\gamma = 0$ the standard deviation seems to be independent of $\tilde{\alpha}$. For $\gamma = \pi$, the slopes of the curves scale roughly as $\tilde{\alpha}^{0.7}\tilde{\beta}^{-0.5}$ at $T = 0$; at $T = 4\hbar^2/mL^2k_B$ the influence of $\tilde{\alpha}$ is very weak and the slopes scale roughly as $\tilde{\beta}^{-0.2}$.

The upper panel of Fig. 11 shows the autocorrelation function of I_S for small and large values of $\tilde{\alpha}$. We see that the effect of increasing $|\tilde{\alpha}|$ is similar to that of lowering the fluctuation temperature. The lower panel of the figure shows the influence of varying $\tilde{\beta}$; the effect of increasing $\tilde{\beta}$ is similar to that of raising the fluctuation temperature.

B. SNS junction

Here we report the results for the case $\alpha = -(\hbar^2/mL^2)\cos(2\pi x/L)$; we take again $\tilde{\beta} = \tilde{R} = 1$. Although taking a value of α that vanishes on the average may look as a drastic change, the results are remarkably similar to those of the previous section.

Figure 12 shows the average deviation of $I_S(\gamma)$ from $I_{S0}(\gamma)$ for the same temperatures as in Fig. 1. We note that in the present case the reduction of I_S is smaller than in the case of a uniform filament. This behavior makes sense, since fluctuations may only be expected to destroy superconductivity

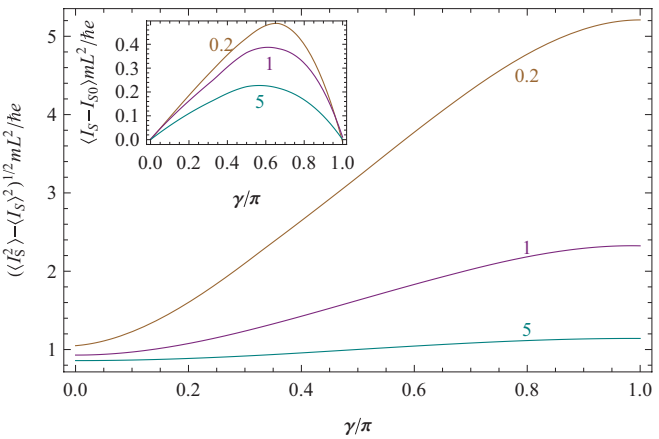

FIG. 9. (Color online) Standard deviation of the supercurrent, as a function of the phase difference, for several values of $\tilde{\beta}$, marked next to each curve. $T = 0.9\hbar^2/mL^2k_B$, $\alpha = -\hbar^2/mL^2$, $\tilde{R} = 1$. Inset: deviation of I_S from I_{S0} for the same parameters.

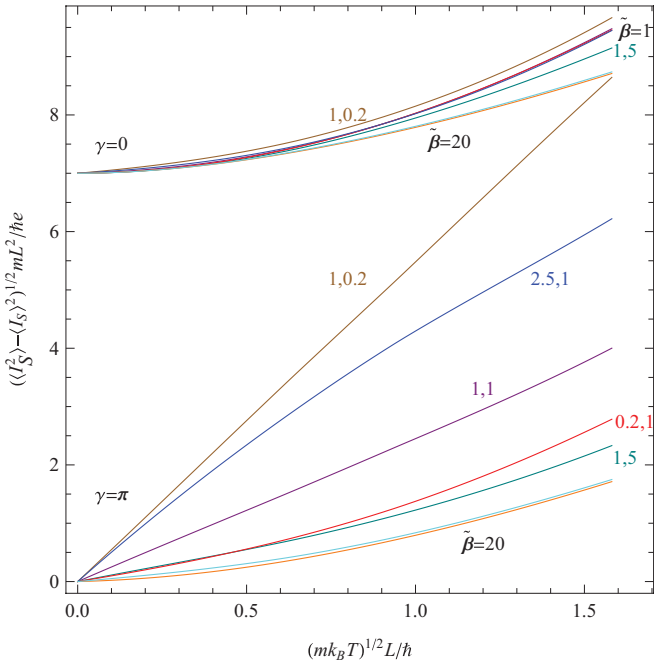

FIG. 10. (Color online) Standard deviation of the supercurrent as a function of temperature, for various values of γ, $\tilde{\alpha}$, and $\tilde{\beta}$. The lower curves are for $\gamma = \pi$ and the curves for $\gamma = 0$ have been raised by 7 units. Most lines are marked by the pair of numbers $|\tilde{\alpha}|$, $\tilde{\beta}$; in cases where $\tilde{\alpha}$ has no visible influence in the graph, only $\tilde{\beta}$ is indicated (for $\tilde{\beta} = 1$, $\tilde{\alpha} = -0.2, -1, -2.5$; for $\tilde{\beta} = 20$, $\tilde{\alpha} = -0.2, -1$).

when the entire filament is superconducting; on the other hand, when half of the filament is normal and supercurrent can only be due to proximity or fluctuations, these fluctuations also have a supportive effect. For $\gamma = \pi$ the average current has to vanish by symmetry; the scattering in this value serves as a measure of the accuracy of our results.

Figure 13 shows the standard deviation of $I_S(\gamma)$ and compares it with that of a uniform filament. For small values of γ the standard deviation is similar to that of Fig. 3, but as γ approaches π the standard deviation in the present case is noticeably smaller than that of a uniform

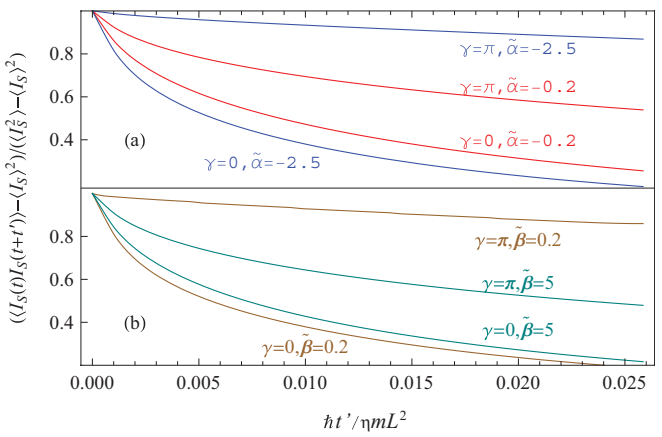

FIG. 11. (Color online) Autocorrelation function of I_S for $T = 0.9\hbar^2/mL^2k_B$, $\tilde{R} = 1$, and various values of γ, $\tilde{\alpha}$, and $\tilde{\beta}$. (a) $\tilde{\beta} = 1$; (b) $\tilde{\alpha} = 1$.

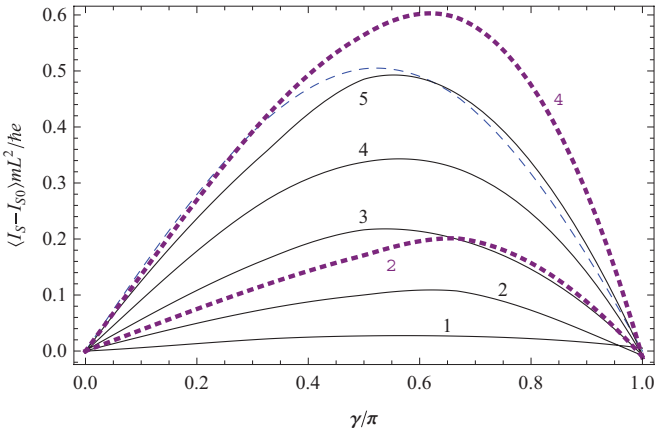

FIG. 12. (Color online) Reduction of average supercurrent due to thermal fluctuations in the case $\alpha = -(\hbar^2/mL^2)\cos(2\pi x/L)$. Annotations as in Fig. 1. For comparison, the curves for $\alpha = -\hbar^2/mL^2$, $T = 0.4\hbar^2/mL^2k_B$, and $T = 1.6\hbar^2/mL^2k_B$ have been included as dotted lines.

filament. This result may seem surprising, since in the present case superconductivity is more fragile and we might expect increased fluctuations. A possible explanation could be that when α and β are both positive, large fluctuations of the order parameter in the middle of the filament are inhibited, leading to smaller fluctuations of I_S. Figure 14 presents these results as functions of the temperature. As in the case of a uniform filament, the standard deviation is not proportional to $T^{1/2}$.

Figure 15 compares the autocorrelation functions for the cases $\alpha(x) = -(\hbar^2/mL^2)\cos(2\pi x/L)$ and $\alpha = -\hbar^2/mL^2$. Again, we find that the difference is remarkably small, especially for small γ. Nominal suppression of superconductivity in part of the filament just leads to a slightly faster decoherence.

IV. DISCUSSION

We have evaluated numerically the thermal fluctuations of the supercurrent along filaments that bridge between two banks (superconducting pieces with dimensions such that

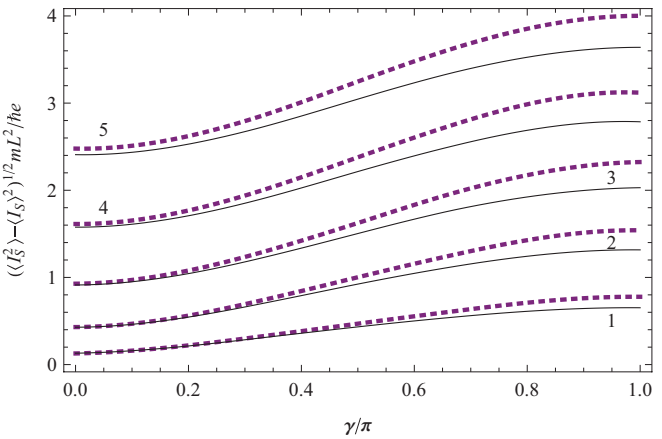

FIG. 13. (Color online) Standard deviation of the supercurrent in the case $\alpha = -(\hbar^2/mL^2)\cos(2\pi x/L)$, for several temperatures. The temperatures are the same as in Fig. 1. For comparison, the curves of Fig. 3 are redrawn as dotted lines.

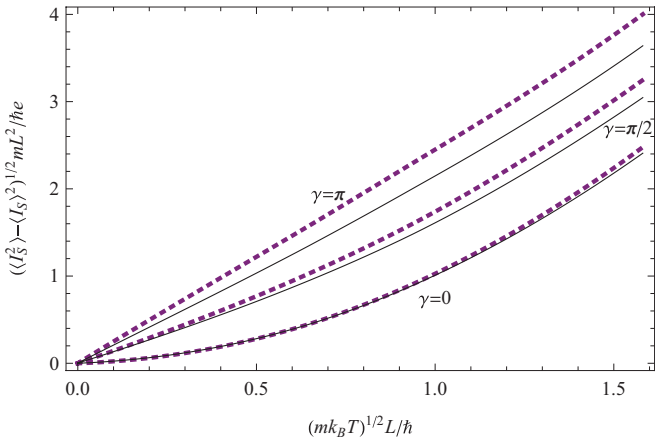

FIG. 14. (Color online) Temperature dependence of the standard deviation of the supercurrent. Solid lines: $\alpha = -(\hbar^2/mL^2)\cos(2\pi x/L)$; dotted: $\alpha = -\hbar^2/mL^2$, redrawn from Fig. 4.

fluctuations in them are negligible) in an equilibrium situation. One case we considered was that of a uniform filament, made of the same material as the banks; the second case was that of a filament equal to the first at the contact points, but normal in the middle.

These fluctuations have nontrivial properties, qualitatively different from those of normal current. Additionally, in spite of the blatant difference between both kinds of considered filaments, the difference between the fluctuations in them is minor, suggesting that the results we have found are generic.

Experimentally, a phase difference may be applied by connecting the banks so that together with the filament they become a closed circuit that encloses a known magnetic flux; the current can then be sensed through the field that it induces. The main signatures of the effects found here are the γ dependencies of the deviation of the average current from I_{S0} and that of the standard deviation of I_S.

I_{S0} could be determined by repetition of the experiment with samples of the same material and length but considerably wider cross section, since I_{S0} is proportional to the cross section.

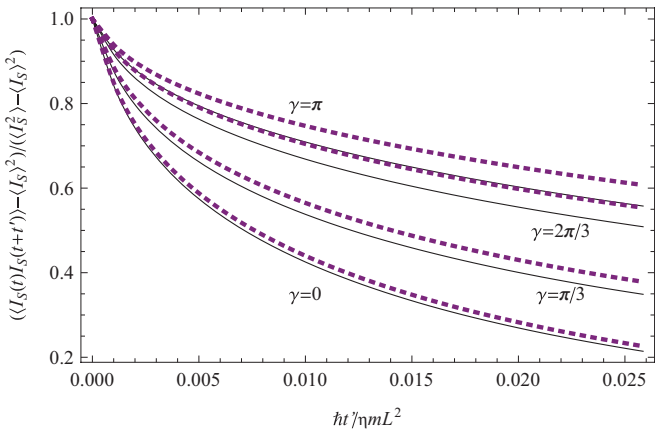

FIG. 15. (Color online) Autocorrelation of the supercurrent, as a function of the elapsed time, for $\alpha = -(\hbar^2/mL^2)\cos(2\pi x/L)$ and several values of γ. The other parameters are as in Fig. 5. The dotted lines are for $\alpha = -\hbar^2/mL^2$.

Increasing w would change the values of $\tilde{\beta}$ and $\tilde{R}$, and as a consequence the value of $\langle I_S\rangle - I_{S0}$ would also increase, but, as shown in Fig. 9, to a much smaller extent.

Let us now discuss measurement of the standard deviation of I_S. The probing time should be of the order of $0.1mL^2/\hbar k_F\ell_e$. This time should be sufficiently large to be experimentally accessible, and also sufficiently larger than $\hbar/k_BT_c$, so that fluctuations of the normal current can be regarded as white noise. This requirement sets a lower bound for L (for $T_c = 10$ K and $k_F\ell_e = 10$, we require $L \gg 10^{-7}$ m). An additional concern is that fluctuations of the supercurrent should not be obscured by those of the normal current. In order to check this possibility, let us examine a situation with $T_c - T$ and w chosen such that $-\tilde{\alpha} = \tilde{\beta} = 1$. According to our results, the standard deviation of I_S for $\gamma = \pi$ will be of the order of $(e/L)(k_BT/m)^{1/2}$. On the other hand, if I_N is measured during periods of time τ, its standard deviation will be $(2k_BT\sigma w/L\tau)^{1/2}$. Using the free electron expression for σ, taking $\tau = 0.1mL^2/\hbar k_F\ell_e$ and w from Eq. (4), we obtain that the standard deviation of I_S is of the same order of magnitude as that of I_N, so that in principle $\langle I_S^2\rangle$ can be determined.

The present study may be regarded as a feasibility test for the influence of supercurrent fluctuations. Analytic treatments that uncover the scalings and asymptotic relations, as well as the nonequilibrium behavior, are still required.

ACKNOWLEDGMENTS

This research was supported by the Israel Science Foundation, Grant No. 249/10. I have benefited from comments from Grzegorz Jung and Baruch Rosenstein.

APPENDIX: EVALUATION OF $\langle I_S\rangle$ USING A TRANSFER OPERATOR TECHNIQUE

The equilibrium average of the supercurrent is given by

$$\langle I_S\rangle = \langle I_S + I_N\rangle = \frac{2\pi k_BT}{\Phi_0}\frac{\partial \ln Z}{\partial\gamma}\,, \tag{A1}$$

where Z is the partition function, which has to be derived from the Ginzburg-Landau free energy

$$F = \int_0^L wds[\alpha|\tilde{\psi}|^2 + (\beta/2)|\tilde{\psi}|^4 + (\hbar^2/2m)|\partial\tilde{\psi}/\partial s|^2]. \tag{A2}$$

For a uniform filament and $\alpha < 0$, writing $s = Lt$ and $(\mathrm{Re}\,\tilde{\psi}, \mathrm{Im}\,\tilde{\psi}) = \sqrt{-\alpha/\beta}\,\mathbf{r}$, F becomes

$$F = -\frac{w\alpha\hbar^2}{L\beta m}\int_0^1 dt\left(\frac{1}{2}\left|\frac{d\mathbf{r}}{dt}\right|^2 + V\right)\,, \tag{A3}$$

with

$$V = (\alpha L^2m/\hbar^2)(r^2 - r^4/2)\,. \tag{A4}$$

Following Ref. 17, a function $\mathbf{r}(t)$ is interpreted as a microstate of the system and F as the energy of the system for that microstate. It follows that the partition function is

$$Z = C\int \mathcal{D}\mathbf{r}\exp(-F/k_BT)\,, \tag{A5}$$

where $\int \mathcal{D}\mathbf{r}$ denotes integration over all functions $\mathbf{r}(t)$ with boundary conditions $\mathbf{r}(0) = \mathbf{a}_0 = (1,0)$ and $\mathbf{r}(1) = \mathbf{a}_1 = (\cos\gamma, \sin\gamma)$, and C is an irrelevant multiplicative constant. Dividing the integral in Eq. (A3) into N segments, $N \gg 1$, and introducing into Eq. (A5) we can write in this limit

$$Z = \left(\frac{N}{2\pi S}\right)^{N-1} \int d\mathbf{r}_1 \cdots d\mathbf{r}_N \delta(\mathbf{r}_1 - \mathbf{a}_0)\delta(\mathbf{r}_N - \mathbf{a}_1) \times \exp\left[-\frac{f(\mathbf{r}_N,\mathbf{r}_{N-1})}{NS}\right] \cdots \exp\left[-\frac{f(\mathbf{r}_2,\mathbf{r}_1)}{NS}\right], \quad \text{(A6)}$$

with $f(\mathbf{r}_{i+1},\mathbf{r}_i) = V(\mathbf{r}_{i+1}) + (N^2/2)|\mathbf{r}_{i+1} - \mathbf{r}_i|^2$, $S = -k_B T L\beta m/w\alpha\hbar^2$, and the prefactor has been chosen for convenience.

Noting that $\delta(\mathbf{r} - \mathbf{r}') = \sum_n \Psi_n^*(\mathbf{r})\Psi_n(\mathbf{r}')$, where $\{\Psi_n\}$ is any complete set of normalized eigenstates, Z becomes

$$Z = \sum_{n,n'} \Psi_{n'}(\mathbf{a}_1)\Psi_n^*(\mathbf{a}_0) \int d\mathbf{r}_N \Psi_{n'}^*(\mathbf{r}_N) \cdots \times \int d\mathbf{r}_i (N/2\pi S) \exp[-f(\mathbf{r}_{i+1},\mathbf{r}_i)/NS] \cdots \times \int d\mathbf{r}_1 (N/2\pi S) \exp[-f(\mathbf{r}_2,\mathbf{r}_1)/NS]\Psi_n(\mathbf{r}_1) . \quad \text{(A7)}$$

If the Ψ_n are chosen so that they obey the eigenvalue equation

$$\int d\mathbf{r}_i (N/2\pi S) \exp[-f(\mathbf{r}_{i+1},\mathbf{r}_i)/NS]\Psi_n(\mathbf{r}_i) = \exp[-\epsilon_n/NS]\Psi_n(\mathbf{r}_{i+1}) , \quad \text{(A8)}$$

then

$$Z = \sum_n \Psi_n(\mathbf{a}_1)\Psi_n^*(\mathbf{a}_0)\exp(-\epsilon_n/S) . \quad \text{(A9)}$$

Expanding $\Psi_n(\mathbf{r}_i)$ in powers of $\mathbf{r}_i - \mathbf{r}_{i+1}$ around $\Psi_n(\mathbf{r}_{i+1})$, which is equivalent to an expansion in powers of $N^{-1/2}$, the integral in Eq. (A8) can be performed and Ψ_n is found to obey the eigenvalue equation[17]

$$[-(S^2/2)\nabla^2 + V]\Psi_n = \epsilon_n \Psi_n , \quad \text{(A10)}$$

where ∇^2 is the Laplacian with respect to $\mathbf{r}$.

In polar coordinates $\mathbf{r} = r(\cos\theta, \sin\theta)$, the angular momentum operator is $L_z = -i\partial/\partial\theta$. Noting that[18] L_z commutes with the "Hamiltonian" $[-(S^2/2)\nabla^2 + V]$, the Ψ_n can be chosen so that they are also eigenstates of L_z, i.e., they can have the form $\Psi_{n,\ell}[r(\cos\theta, \sin\theta)] = R_{n,\ell}(r)\exp(i\ell\theta)$, where $R_{n,\ell}$ is a real function and ℓ an integer. Introducing this form into Eq. (A9) we obtain

$$Z = \sum_\ell \exp(i\ell\gamma) Z_\ell , \quad \text{(A11)}$$

with

$$Z_\ell = \sum_n R_{n,\ell}^2(1)\exp(-\epsilon_{n,\ell}/S) , \quad \text{(A12)}$$

where summation in Eq. (A11) is made over all integers and in Eq. (A12) over all the states with total angular momentum ℓ.

Since the Hamiltonian is symmetric under the transformation $\mathbf{r} \to -\mathbf{r}$, we can also write

$$Z = Z_0 + 2\sum_{\ell=1}^{\infty} \cos(\ell\gamma) Z_\ell . \quad \text{(A13)}$$

Applying Eq. (A1) we obtain

$$\langle I_S \rangle = -\frac{4\pi k_B T}{\Phi_0 Z} \sum_{\ell=1}^{\infty} \sin(\ell\gamma)\ell Z_\ell . \quad \text{(A14)}$$

In order to complete the evaluation, Eqs. (A14) and (A12) have to be supplemented with the values of $\epsilon_{n,\ell}$ and $R_{n,\ell}(1)$. Since only for small values of $\epsilon_{n,\ell}$ is there an appreciable contribution, this is accomplished as follows. We start from a basis Hamiltonian $H_B = -(S^2/2)\nabla^2 + (k^2/2)r^2$, which has known eigenfunctions $R_{n,\ell}^B(r) = C_{n,\ell} r^{|\ell|} e^{-kr^2/2S}\, {}_1F_1(-n, |\ell| + 1, kr^2/S)$ and eigenvalues $\epsilon_{n,\ell}^B = Sk(2n + |\ell| + 1)$, where $C_{n,\ell}$ is the normalization constant and ${}_1F_1$ is Kummer's hypergeometric function. k is still a free parameter. We select a subspace of the Hilbert space which has a moderate number of low-energy eigenstates of H_B as a basis, project the true Hamiltonian into this subspace, and then diagonalize this truncated Hamiltonian.

The value of k is chosen as follows. If the Hamiltonian were not truncated, its lowest eigenvalue would be independent of k; for the truncated Hamiltonian and for a given value ℓ,

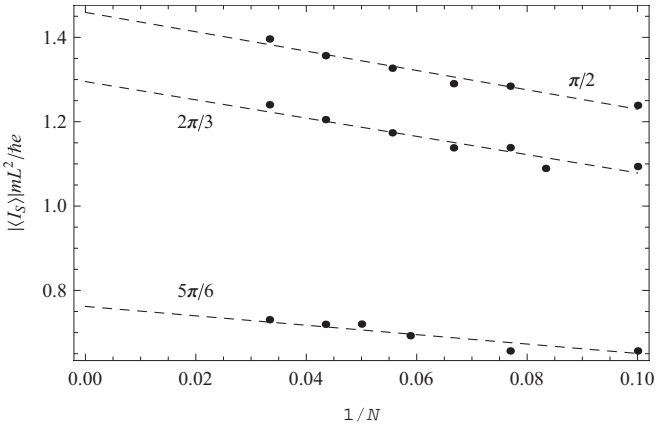

FIG. 16. Supercurrent as a function of the length of the computational segments. The dashed lines extrapolate to the values obtained by the method described in this appendix. The temperature is $2.5\hbar^2/mL^2k_B$, the phase difference is marked next to each line and the other parameters are as in Fig. 1. We kept 12 terms in expansion (A14).

the lowest eigenvalue is effectively independent of k within a certain range and rises beyond this range. We choose $k(\ell)$ in the middle of this range.

Figure 16 compares the computational method taken from Refs. 10,11 and the method developed in this appendix. The comparison requires extrapolation to the continuum limit, $N \to \infty$. The convergence of $\langle I_S \rangle$ to the continuum limit is rather slow, but the variance of I_S seems to saturate for $N \sim 20$. For temperatures lower than $0.4\hbar^2/mL^2k_B$ convergence in Eq. (A14) becomes slow.

*jorge.berger@braude.ac.il

[1] M. Tinkham, *Introduction to Superconductivity* (McGraw-Hill, New York, 1996).

[2] K. K. Likharev, *Dynamics of Josephson Junctions and Circuits* (Gordon and Breach, New York, 1986).

[3] A. Barone and G. Paternò, *Physics and Applications of the Josephson Effect* (Wiley, New York, 1982).

[4] Yu. M. Ivanchenko and L. A. Zil'berman, Sov. Phys. JETP **28**, 1272 (1969) [Zh. Eksp. Teor. Fiz. **55**, 2395 (1968)].

[5] V. Ambegaokar and B. I. Halperin, Phys. Rev. Lett. **22**, 1364 (1969); **23**, 274(E) (1969).

[6] D. Rogovin and D. J. Scalapino, Ann. Phys. (NY) **86**, 1 (1974).

[7] D. Averin and H. T. Imam, Phys. Rev. Lett. **76**, 3814 (1996).

[8] A. Baratoff, J. A. Blackburn, and B. B. Schwartz, Phys. Rev. Lett. **25**, 1096 (1970); **25**, 1738(E) (1970).

[9] K. K. Likharev and L. A. Yakobson, Sov. Phys. JETP **41**, 570 (1976) [Zh. Eksp. Teor. Fiz. **68**, 1150 (1975)].

[10] J. Berger, Phys. Rev. B **75**, 184522 (2007).

[11] J. Berger, J. Phys.: Condens. Matter **23**, 225701 (2011).

[12] G. Richardson and J. Rubinstein, Proc. R. Soc. London A **455**, 2549 (1999).

[13] L. P. Gor'kov and G. M. Eliashberg, Sov. Phys. JETP **27**, 328 (1968) [Zh. Eksp. Teor. Fiz. **54**, 612 (1968)].

[14] L. Kramer and R. J. Watts-Tobin, Phys. Rev. Lett. **40**, 1041 (1978); R. J. Watts-Tobin, Y. Krähenbühl, and L. Kramer, J. Low Temp. Phys. **42**, 459 (1981).

[15] A. Crassous, R. Bernard, S. Fusil, K. Bouzehouane, D. LeBourdais, S. Enouz-Vedrenne, J. Briatico, M. Bibes, A. Barthelemy, and J. E. Villegas, Phys. Rev. Lett. **107**, 247002 (2011) and references therein.

[16] J. Berger, Phys. Rev. B **70**, 024524 (2004).

[17] D. J. Scalapino, M. Sears, and R. A. Ferrell, Phys. Rev. B **6**, 3409 (1972).

[18] F. von Oppen and E. K. Riedel, Phys. Rev. B **46**, 3203 (1992).